



# Parameter design of governor power system stabilizer to suppress ultra-low-frequency oscillations based on phase compensation

Xin Zhou<sup>1</sup> · Muhammad Usman<sup>2</sup> · Peng He<sup>1</sup> · Muhammad Shahid Mastoi<sup>2</sup> · Shaobo Liu<sup>2</sup>

Received: 2 December 2019 / Accepted: 27 August 2020 / Published online: 24 September 2020  
© Springer-Verlag GmbH Germany, part of Springer Nature 2020

## Abstract

In a few of the isolated DC power-transmission systems with hydropower units (and the associated water hammer effect), inappropriate governor control parameters may weaken the system damping and stability. It has the potential to result in ultra-low-frequency oscillations (ULFO) which is below 0.1 Hz. To carry out this issue, a linearized state-space model of a multi-machine system that includes hydropower and steam turbine governor control systems is presented in this paper. The oscillation mode of ULFO about the damping characteristics of the governor control system is analyzed by the damping torque analysis method. A governor power system stabilizer (GPSS) design model predicated on phase compensation principle to heighten the damping of the governor control system to subdue ULFO is planned. To verify its effectiveness, the designed GPSS is applied to a single-machine system, a 4-machine 2-area system as well as the Yunnan power grid system of China. The simulation results demonstrate that GPSS effectively suppresses ULFO with heightened ULFO damping by the optimized settings of governor control parameters.

**Keywords** ULFO · Characteristic analysis method · Damping torque analysis method · Phase compensation principle · GPSS

## 1 Introduction

By interconnection of power systems, the stability of a large-scale power system becomes more important and challenging. Usually, the electric power stations and sources are far away from the load centers [1]. In a power system, power generation (turbines, generators) and loads (consumption) are interconnected through a network, of various power equipment and transmission lines (AC as well as DC lines). Power system is continually exposed to instabilities, such as fluctuations of load and line breakdown. It happens due to different reasons like low- or ultra-low-frequency oscillations (LFO and ULFO, respectively, 0.1–2.0 Hz is LFO, below 0.1 Hz is ULFO). Hydropower has an important role in the safe, stable, and efficient operation of the electric power system. Supply of stable and balanced electric power during such instabilities, proper operations of a controller, such

as an excitation system or a governor are required. In sizeable power systems, wide-ranging low-frequency oscillation (LFO) threatens the operational stability. So exact assessment and suppression of the dominant oscillation mode are some of the important factors for the steady and stable operation of the system. In the power system, oscillation occurs generally in low and ultra-low-frequency ranges [2–4].

In recent years, with the widespread applications of huge-capacity, long-distance DC transmission technologies in real power grids, some ultra-low-frequency oscillation phenomena with oscillation frequencies below 0.1 Hz have arisen [5–10]. As ULFO is not a relative oscillation between the generator rotors, but the frequency oscillation in the primary frequency modulation process triggered by small system disturbances, it is a power system frequency stability issue [11]. Hydropower units in the Yunnan power grid contribute about 71–75% of the total output. When a power disturbance occurs, the water hammer effect of the hydropower turbine increases the active power imbalance, which leads to instability of grid frequency. In April 2016, when an asynchronous connection test was performed to connect the Yunnan power grid to China Southern Power Grid (main grid), a ULFO arose in the Yunnan power grid with an oscillation frequency of 0.05 Hz and amplitude of 0.1 Hz. The interconnection of

✉ Muhammad Usman  
muhammadusman@my.swjtu.edu.cn

<sup>1</sup> Yunnan Electrical Power Research Institute, Kunming 650217, Yunnan, China

<sup>2</sup> School of Electrical Engineering, Southwest Jiaotong University, Sichuan 610031, Chengdu, China

regional power grids is becoming more and more compact. As the grid operates in a variety of ways, the occurrence of low-frequency oscillations will have a serious impact on the grid. As the primary frequency regulation function of a significant power plant ended, the oscillation gradually vanished [12–14]. To ensure the secure and steady operation of power system grids, it is of huge value to analyze the oscillation characteristics and the suppression measures of ULFOs arising in the system.

In Refs. [15, 16], the Nyquist curve of the primary frequency modulation model was used to expose the mechanism of ULFO. The influence of governor PID parameters on system stability was analyzed with the Routh–Hurwitz criterion. The stability analysis of the hydropower units has also been performed. In Refs. [17, 18], the proportional-integral-derivative (PID) controller is widely used in the power system with the characteristics of a simple structure and strong robustness. Reference [19] describes that the hydraulic turbine governing system (HTGS) is the main controlling system of hydropower production units. References [11, 20] introduced the dynamic characteristics of the hydropower governor in detail. References [21, 22] pointed out that the governor system's control method is ULFO mode, with the damping ratio often affected by the PID parameters. The ULFO was a non-electromechanical oscillation mode in the Yunnan power grid. Optimizing the governor's PID parameters could effectively increase the system stability. In Ref. [23], a relevant coefficient index (RCI) was proposed to screen the generator units with high sensitivity to ULFO. The governor's PID parameters of the sensitive generators were optimized to suppress ULFO. Reference [24] proposed a method to optimize the governor's parameters, where the optimization's constraint was the damping torque of the prime mover in the entire oscillation frequency range. The optimization objective was the integral of the time-weighted-absolute-error (ITAE) of prime mover's step response under different load conditions. The optimized parameters effectively ensured the system stability under different conditions. Right now, at most the ULFO is suppressed by tuning the PID parameters of the governor control system. But the effect is subject to system operating conditions as well as the specific PID parameter optimization method itself. At the same time, tuning the PID parameters of the governor control system may hurt some low-frequency oscillation modes. Reference [25] describes that a PID governor controller design based on the particular operational conditions does not always ensure the provision of acceptable performance over a wide-range of conditions. In Ref. [26], a field test was performed on the hydropower units, with governor power system stabilizer (GPSS) to verify that GPSS could increase the stability of

the units. In Ref. [27], the power system experiences persistent low-frequency oscillation in the transmission lines after being troubled due to the lack of damping. In recent years, many research results of damping control strategies are available. Reference [28] to analyze small-signal dynamics damping torque analysis is an imperative technique. Reference [25] states that an appropriate tuning of governor offers an enhanced damping of the system oscillations along with increased system robustness. References [29, 30] analyzed the damping characteristics of large and small disturbances under the additional damping control of GPSS. It is completely performed in a single-machine infinity system as well as a multi-machine system. The results showed the efficacy of GPSS for both large and small disturbances. Reference [31] proposed an adaptive governor power system stabilizer (AGPSS) with multi-machine decoupling characteristics, which could suppress low-frequency oscillation in the single-machine infinite system as well as a multi-machine system.

Keeping in view the previous works, in this paper, at first the ULFO mode was solved based on the linearized state-space model of the multi-machine system that contains hydropower and steam turbine governor control systems before the ULFO was analyzed in the 4-machine 2-area system according to the participation factor and the root locus. The damping characteristics of the PID-type governor control system were then analyzed using the damping torque analysis method and a GPSS design method to suppress ULFO based on the phase compensation principle.

Finally, the suggested method is verified by the simulations with a single-machine, single-load system and the 13 main hydropower plants of the Yunnan power grid with large rated capacities. The mechanical damping provided by GPSS is not affected by the operating mode and conditions on the grid side. On top of the advantages of simple design, easy debug and calculation, GPSS damping has no negative impact on low-frequency oscillation mode in the system. Therefore, it could be of great value to guarantee the safe and stable operation of power system grids.

In this paper, the model linearization is established in Sect. 2. Section 3 is a description of GPSS design based on the phase compensation principle, where the principle of ULFO suppression and parameter tunings of the single- and multi-machine systems are stated. Section 4 presents analysis and verification of state-space model, analysis of the mechanical damping torque coefficient, Sensitivity analysis of ULFO mode, Influence of governor system model parameters on eigenvalues and ULFO in the actual power grid are explained. Finally, in Sect. 5 some conclusions are drawn.

## 2 Model linearization including hydrogenerator and steam turbine generator

A linearized state-space model for multi-machine systems is established here. Considering the saliency pole effect of the generator and the excitation system dynamic, a practical third-order model is adopted for the generator, and the static excitation system is represented with a first-order inertial element. The small disturbance models of the generator and excitation system are

$$\begin{cases} \Delta \dot{\delta} = \omega_0 \Delta \omega \\ M \Delta \dot{\omega} = \Delta P_m - \Delta P_e - D \Delta \omega \\ T'_{d0} \Delta \dot{E}'_q = \Delta E'_{fd} - \Delta E_q \\ T_A \Delta \dot{E}'_{fd} = -\Delta E'_{fd} - K_A \Delta V \end{cases} \quad (1)$$

where  $\Delta \delta$  is the rotor angular increment of the generator;  $\Delta \omega$  is the angular speed increment of the generator;  $\omega_0$  is the reference angular frequency of the system;  $M$  is the inertia time constant of the generator;  $D$  is the damping coefficient of the generator;  $\Delta P_m$  is the mechanical power increment of the generator;  $\Delta P_e$  is the electromagnetic power increment of the generator;  $T'_{d0}$  is the time constant of the exciting winding itself;  $\Delta E_q$  is the idle electromotive force increment of the actual exciting current;  $\Delta E'_q$  is the quadrature-axis transient electromotive force increment of the generator;  $\Delta E'_{fd}$  is the output voltage increment of the excitation system;  $K_A$  and  $T_A$  are the gain and the time constant of the excitation system, respectively;  $\Delta V$  is the actual terminal voltage increment of the generator.

### (a) Model of hydrogenerator units

To study ULFO, a relatively complicated hydropower governor control system model is selected, which consists of the governor system model (GM/GM+), the electro-hydraulic servo system model (GA) and the prime mover model (TW) in PSD-BPA software. In actual operation and control of power system, the differential and integral coefficients of the PID governor of hydrosystem hardly affect its dynamic characteristics. For the sake of simplicity, usually their values are set to 0. Such a linearized model of the hydroturbine and governing system is shown in Fig. 1 where  $K_W$  is the gain of the frequency deviation;  $B_P$  is the permanent speed droop;  $K_{P1}$  is the proportional gain of the governor system;  $K_{I1}$  is the integral gain of the governor system;  $K_{P2}$  is the proportional gain of the servo system;  $T_{CO}$  is the closing or opening time constant of the hydraulic servo-motor;  $T_2$  is the time constant of the feedback element of the hydraulic servo-motor; and  $T_W$  is the time constant of the water hammer effect.

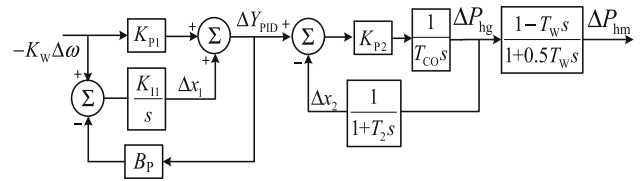


Fig. 1 Linearized model of a hydropower governor control system

According to the linearized model shown in Fig. 1, the transfer function of the hydropower system is

$$G_{ht}(s) = \frac{1 - T_W s}{1 + 0.5 T_W s} \quad (2)$$

Opening feedback element of the servo system almost does not participate in the ULFO, and its time constant does not affect the characteristics of ULFO, for simplicity,  $T_2 = 0$ . Now the transfer function of the governor system is

$$G_{hg}(s) = \frac{K_W (K_{P1} + K_{I1}/s)}{1 + K_{I1} B_P/s} \frac{1}{1 + T_{CO} s / K_{P2}} \quad (3)$$

According to Eqs. (2) and (3), the transfer function of the hydroturbine prime mover system is

$$G_{hm}(s) = G_{hg}(s) G_{ht}(s) \quad (4)$$

Taking the state variables of the integral element output of governor system as  $\Delta x_1$ , the opening feedback element output of the servo system as  $\Delta x_2$ , the governor valve opening as  $\Delta P_{hg}$ , and the mechanical power as  $\Delta P_{hm}$ , the small disturbance models of the hydroturbine and the governor system are

$$\begin{cases} \Delta \dot{P}_{hm} = \frac{2K_W K_{P1} K_{P2}}{T_{CO}} \Delta \omega - \frac{2}{T_W} \Delta P_{hm} + \frac{2}{T_W} \Delta P_{hg} \\ \quad - \frac{2K_{P2}}{T_{CO}} \Delta x_1 + \frac{2K_{P2}}{T_{CO}} \Delta x_2 \\ \Delta \dot{P}_{hg} = \frac{K_W K_{P1} K_{P2}}{T_{CO}} \Delta \omega + \frac{K_{P2}}{T_{CO}} \Delta x_1 - \frac{K_{P2}}{T_{CO}} \Delta x_2 \\ \Delta \dot{x}_1 = (B_P K_W K_{P1} K_{I1} - K_W K_{I1}) \Delta \omega - B_P K_{I1} \Delta x_1 \\ \Delta \dot{x}_2 = \frac{1}{T_2} \Delta P_{hg} - \frac{1}{T_2} \Delta x_2 \end{cases} \quad (5)$$

### (b) Model of steam turbine generator units

The selected steam turbine governor control system model consists of a governor model (GS) and a prime mover model (TB). The linearized model is shown in Fig. 2,  $R$  is the permanent speed droop;  $T_C$  is the servo time constant;  $T_{CH}$ ,  $T_{RH}$ , and  $T_{CO}$  are the time constants of the steam chest, reheater, and crossover duct, respectively;  $F_{HP}$ ,  $F_{IP}$ , and  $F_{LP}$  are the power ratio coefficients of the high-, medium-, and low-pressure cylinders, respectively.

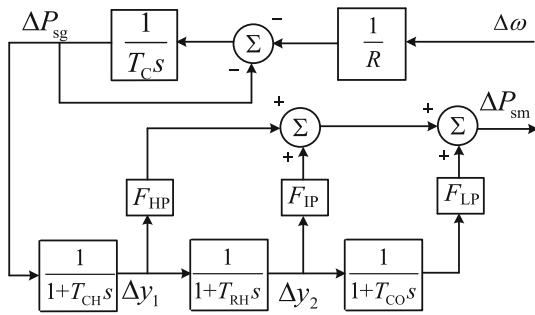


Fig. 2 Linearized model of steam turbine governor control system

Setting  $F_{LP} = 0$ , the transfer function of the steam turbine primary system is obtained.

$$G_{sm}(s) = \frac{1}{R} \frac{1}{1 + T_C s} \frac{1 + F_{HP} T_{RH} s}{(1 + T_{CH} s)(1 + T_{RH} s)} \quad (6)$$

Take the state variables as  $\Delta y_1$ ,  $\Delta y_2$ ,  $\Delta P_{sg}$ , and  $\Delta P_{sm}$ , the small disturbance models of the steam turbine and the governor system are

$$\begin{cases} \Delta \dot{P}_{sm} = F_{HP} \Delta y_1 + F_{IP} \Delta y_2 \\ \Delta \dot{P}_{sg} = -\frac{1}{RT_C} \Delta \omega - \frac{1}{T_C} \Delta P_{sg} \\ \Delta \dot{y}_1 = \frac{1}{T_{CH}} \Delta P_{sg} - \frac{1}{T_{CH}} \Delta y_1 \\ \Delta \dot{y}_2 = \frac{1}{T_{RH}} \Delta y_1 - \frac{1}{T_{RH}} \Delta y_2 \end{cases} \quad (7)$$

Including multiple hydrogenerator and steam turbine generator models, according to the linearized models of the generator–excitation system, the load–governor control system and taking the derivation process of the linearized model of multi-machine system as a reference, keep the state variables  $\Delta \delta$ ,  $\Delta \omega$ ,  $\Delta E'_q$ ,  $\Delta E'_{fd}$ ,  $\Delta P_{hm}$ ,  $\Delta P_{sg}$ ,  $\Delta P_{sm}$ ,  $\Delta P_{hg}$ ,  $\Delta x_1$ ,  $\Delta x_2$ ,  $\Delta y_1$ , and  $\Delta y_2$ , but use state variables to represent  $\Delta P_e$ ,  $\Delta E_q$ , and  $\Delta V$ . The linearized state-space equation of the multi-machine system is

$$\begin{bmatrix} \Delta \dot{\delta} \\ \Delta \dot{\omega} \\ \Delta \dot{E}'_q \\ \Delta \dot{E}'_{fd} \\ \Delta \dot{P}_{hm} \\ \Delta \dot{P}_{sm} \\ \Delta \dot{P}_{hg} \\ \Delta \dot{P}_{sg} \\ \Delta \dot{x}_1 \\ \Delta \dot{x}_2 \\ \Delta \dot{y}_1 \\ \Delta \dot{y}_2 \end{bmatrix} = \begin{bmatrix} 0 & A_{12} & 0 & 0 & 0 & 0 & 0 & 0 & 0 & 0 & 0 & 0 \\ A_{21} & A_{22} & A_{23} & 0 & M_h^{-1} & M_s^{-1} & 0 & 0 & 0 & 0 & 0 & 0 \\ A_{31} & 0 & A_{33} & A_{34} & 0 & 0 & 0 & 0 & 0 & 0 & 0 & 0 \\ A_{41} & 0 & A_{43} & A_{44} & 0 & 0 & 0 & 0 & 0 & 0 & 0 & 0 \\ 0 & 2X_1 & 0 & 0 & -2X_2 & 0 & 2X_2 & 0 & -2X_3 & 2X_3 & 0 & 0 \\ 0 & 0 & 0 & 0 & 0 & 0 & 0 & 0 & 0 & 0 & F_{HP} & F_{IP} \\ 0 & -X_1 & 0 & 0 & 0 & 0 & 0 & 0 & X_3 & -X_3 & 0 & 0 \\ 0 & Y_1 & 0 & 0 & 0 & 0 & 0 & 0 & Y_2 & 0 & 0 & 0 \\ 0 & X_4 & 0 & 0 & 0 & 0 & 0 & 0 & X_5 & 0 & 0 & 0 \\ 0 & 0 & 0 & 0 & 0 & 0 & X_6 & 0 & 0 & -X_6 & 0 & 0 \\ 0 & 0 & 0 & 0 & 0 & 0 & 0 & 0 & Y_3 & 0 & 0 & -Y_3 \\ 0 & 0 & 0 & 0 & 0 & 0 & 0 & 0 & 0 & 0 & Y_4 & -Y_4 \end{bmatrix} \begin{bmatrix} \Delta \delta \\ \Delta \omega \\ \Delta E'_q \\ \Delta E'_{fd} \\ \Delta P_{hm} \\ \Delta P_{sm} \\ \Delta P_{hg} \\ \Delta P_{sg} \\ \Delta x_1 \\ \Delta x_2 \\ \Delta y_1 \\ \Delta y_2 \end{bmatrix} \quad (8)$$

where

$$\begin{bmatrix} 0 & A_{12} & 0 & 0 \\ A_{21} & A_{22} & A_{23} & 0 \\ A_{31} & 0 & A_{33} & A_{34} \\ A_{41} & 0 & A_{43} & A_{44} \end{bmatrix} = \begin{bmatrix} 0 & \omega_0 I & 0 & 0 \\ -M^{-1} K_1 & -M^{-1} D & -M^{-1} K_2 & 0 \\ -T'_{d0}{}^{-1} K_4 & 0 & -T'_{d0}{}^{-1} K_3 & T'_{d0}{}^{-1} \\ -T_A^{-1} K_A K_5 & 0 & -T_A^{-1} K_A K_6 & -T_A^{-1} \end{bmatrix}$$

and  $K_1$ – $K_6$  are the coefficient matrices reflecting the component parameters, grid structure, load characteristics, and operating conditions;  $X_1$ – $X_6$  and  $Y_1$ – $Y_4$  are the system matrices under the governor control system, and  $X_1 = \text{diag}(K_W K_{P1} K_{P2} / T_{CO})$ ,  $X_2 = \text{diag}(1/T_W)$ ,  $X_3 = \text{diag}(K_{P2} / T_{CO})$ ,  $X_4 = \text{diag}(B_P K_W K_{P1} K_{I1} - K_W K_{I1})$ ,  $X_5 = \text{diag}(-B_P K_{I1})$ ,  $X_6 = \text{diag}(1/T_2)$ ,  $Y_1 = \text{diag}(-1/RT_C)$ ,  $Y_2 = \text{diag}(-1/T_C)$ ,  $Y_3 = \text{diag}(-1/T_{CH})$ , and  $Y_4 = \text{diag}(-1/T_{RH})$ , respectively.

The eigenvalues of the ULFO mode appear in the form of conjugate pairs, i.e.,

$$\lambda = \sigma \pm j\omega \quad (9)$$

The oscillation frequency is

$$f = \frac{\omega}{2\pi} \quad (10)$$

The damping ratio is

$$\zeta = -\frac{\sigma}{\sqrt{\sigma^2 + \omega^2}} \quad (11)$$

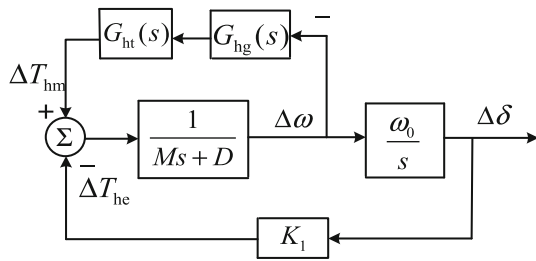


Fig. 3 Frequency regulation model of the governor control system

Based on the linearized state-space model of a multi-machine system, the eigenvalues of the ULFO mode are calculated. The oscillation frequency  $\omega_S$  and the damping ratio  $\zeta_S$  can be obtained according to Eqs. (9)–(11).

### 3 GPSS design based on the phase compensation principle

#### 3.1 Principle of ULFO suppression by GPSS

The high hydropower proportion can lead to ULFOs in the system. Therefore, in this section, a frequency regulation model of a hydropower governor control system is established in Fig. 3, based on which the principle of ULFO suppression by GPSS is analyzed using the damping torque method.

Since the system rotational speed changes little during the transient process, i.e.,  $\omega \approx 1$  p.u.,  $\Delta P_m \approx \Delta T_m$  and  $\Delta P_e \approx \Delta T_e$ . The incremental equations of the rotor motion of the generator can be expressed with the first two equations of Eq. (1). When the angular frequency of the system oscillation is  $\omega_S$ , the first equation of Eq. (1) is written as

$$\Delta\omega = j \frac{\omega_S}{\omega_0} \Delta\delta. \tag{12}$$

When the angular frequency of the mechanical oscillation is  $\omega_S$ , the mechanical power increment  $\Delta P_{hm}$  of the hydropower governor control system is;

$$\begin{aligned} -\Delta P_{hm} &= \bar{G}_{hm}(j\omega_S)\Delta\omega \\ &= \text{Re}[\bar{G}_{hm}(j\omega_S)]\Delta\omega + j\text{Im}[\bar{G}_{hm}(j\omega_S)]\Delta\omega \\ &= \text{Re}[\bar{G}_{hm}(j\omega_S)]\Delta\omega - \frac{\omega_S}{\omega_0}\text{Im}[\bar{G}_{hm}(j\omega_S)]\Delta\delta \\ &= K_D\Delta\omega + K_S\Delta\delta \end{aligned} \tag{13}$$

where  $K_D$  is the mechanical damping torque coefficient and  $K_S$  is the mechanical synchronous torque coefficient.

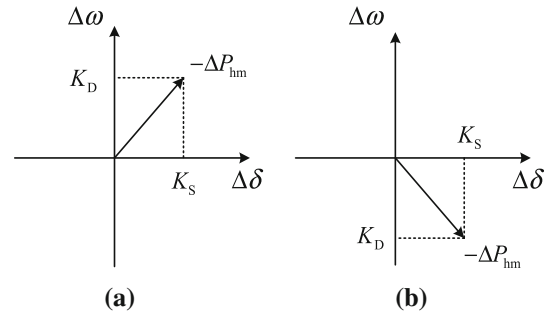


Fig. 4 Vector diagram of mechanical torque

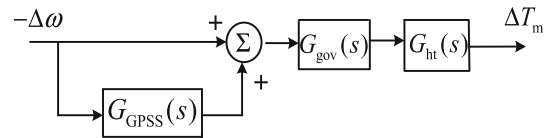


Fig. 5 Block diagram of the governor control system with GPSS

The relationship between ULFO damping ratio  $\zeta_S$  and total mechanical damping torque  $K_D$  satisfies [11]

$$\zeta_S = \frac{D + K_D}{2M\omega_n} = \frac{D + K_D}{2\sqrt{K_S M \omega_0}} \tag{14}$$

where  $\omega_n$  is the angular frequency of the undamped natural oscillation.

In the  $\Delta\delta - \Delta\omega$  coordinate system, the vector diagram of mechanical torque is drawn in Fig. 4. When  $-\Delta P_{hm}$  falls in the first quadrant,  $K_D > 0$ , and the positive damping torque provided by the governor system is shown in Fig. 4a. When  $-\Delta P_{hm}$  falls in the 4th quadrant,  $K_D < 0$ , and the negative damping torque provided by the governor system is shown in Fig. 4b. In the hydropower governor system,  $G_{hg}(s)$  and  $G_{ht}(s)$  are both lag elements, which make  $-\Delta P_{hm}$  lag behind  $\Delta\omega$  in phase. When a ULFO occurs in the system, the hydropower governor control system provides negative damping, so that  $-\Delta P_{hm}$  falls in the 4th quadrant.

In this paper, a GPSS that has a similar structure and transfer function to a power system stabilizer (PSS) is introduced into the governor control system. The transfer function is

$$G_{GPSS}(s) = K_{GPSS} \frac{1 + sT_2}{1 + sT_1} \frac{1 + sT_4}{1 + sT_3} \tag{15}$$

where  $T_2 > T_1 > 0$ ,  $T_4 > T_3 > 0$ , and  $K_{GPSS} > 0$ .

In the governor control model with GPSS as shown in Fig. 5, the GPSS generates the leading phase to reduce the phase lag  $-\Delta P_{hm}$  concerning  $\Delta\omega$ . As a result, the mechanical damping torque coefficient of the governor control system and the system damping ratio both increase to help suppress ULFO.

### 3.2 GPSS parameters tuning

#### 3.2.1 GPSS parameter tunings in a single-machine system

Using the phase compensation method to tune the GPSS parameters in a single-machine system is straightforward, easy to debug and involves fewer calculations. From Fig. 5, the mechanical torque provided by GPSS is

$$\Delta T_{GPSS} = -G_{GPSS}(s)G_{hm}(s)\Delta\omega \tag{16}$$

The mechanical torque provided by GPSS under the angular frequency  $\omega_s$  can be decomposed as follows:

$$\begin{aligned} \Delta T_{GPSS} &= -\bar{G}_{GPSS}(j\omega_s)\bar{G}_{hm}(j\omega_s)\Delta\omega \\ &= -\text{Re}[\bar{G}_{GPSS}(j\omega_s)\bar{G}_{hm}(j\omega_s)]\Delta\omega \\ &\quad + \frac{\omega_s}{\omega_0}\text{Im}[\bar{G}_{GPSS}(j\omega_s)\bar{G}_{hm}(j\omega_s)]\Delta\delta \\ &= T_{GPSSD}\Delta\omega + T_{GPSSS}\Delta\delta \end{aligned} \tag{17}$$

where  $T_{GPSSD}$  and  $T_{GPSSS}$  are the damping torque coefficient and the synchronous torque coefficient, respectively. For an efficient design, GPSS should ideally provide only positive damping torque, i.e.,

$$\Delta T_{GPSS} = D_{GPSS}\Delta\omega, \quad D_{GPSS} < 0 \tag{18}$$

where  $D_{GPSS}$  is the desired damping torque coefficient provided by GPSS. From Eqs. (17) and (18),  $D_{GPSS}$  should satisfy

$$D_{GPSS} = -\text{Re}[\bar{G}_{GPSS}(j\omega_s)\bar{G}_{hm}(j\omega_s)]. \tag{19}$$

According to Eq. (19), the phase angle of GPSS should be set to cancel out the forward path phase angle  $\bar{G}_{hm}(j\omega_s)$ . The objective of the GPSS parameter tuning is to compensate for the phase lag of the forward path, ensuring a positive net damping torque. Equation (19) represents the phase-compensation-based GPSS parameters tuning method. Only if

$$\begin{cases} \bar{G}_{hm}(j\omega_s) = |G_{hm}| \angle \phi \\ \bar{G}_{GPSS}(j\omega_s) = |G_{GPSS}| \angle \gamma \end{cases} \tag{20}$$

where

$$\begin{cases} |G_{hm}| = \sqrt{(\text{Re}[\bar{G}_{hm}(j\omega_s)])^2 + (\text{Im}[\bar{G}_{hm}(j\omega_s)])^2} \\ \phi = \arctan \frac{\text{Im}[\bar{G}_{hm}(j\omega_s)]}{\text{Re}[\bar{G}_{hm}(j\omega_s)]} \end{cases} \tag{21}$$

Substituting  $s = j\omega_s$  into Eq. (4) yields

$$\begin{cases} \text{Re}[\bar{G}_{hm}(j\omega_s)] = A(a_1\omega_s^4 + a_2\omega_s^2 + a_3) \\ \text{Im}[\bar{G}_{hm}(j\omega_s)] = A(b_1\omega_s^5 + b_2\omega_s^3 + b_3\omega_s) \\ A = [(\omega_s^2 + K_{I1}^2 B_P^2)(1 + T_{CO}^2 \omega_s^2 / K_{P2}^2)(1 + 0.25T_W^2 \omega_s^2)]^{-1} \end{cases} \tag{22}$$

where

$$\begin{cases} a_1 = -0.5K_W K_{P1} T_W^2 - 1.5K_W K_{P1} T_W T_{CO} / K_{P2} \\ \quad - 0.5(K_W K_{P1} K_{I1} B_P - K_W^2 K_{P1} K_{I1}) T_W^2 T_{CO} / K_{P2} \\ a_2 = K_W K_{P1} + 1.5(K_W K_{P1} K_{I1} B_P - K_W^2 K_{P1} K_{I1}) T_W \\ \quad - 0.5K_W^2 K_{P1} K_{I1}^2 B_P T_W^2 \\ \quad + (K_W K_{P1} K_{I1} B_P - K_W^2 K_{P1} K_{I1}) T_{CO} / K_{P2} \\ \quad - 1.5K_W^2 K_{P1} K_{I1}^2 B_P T_{CO} T_W / K_{P2} \\ a_3 = K_W^2 K_{P1} K_{I1}^2 B_P \\ b_1 = 0.5K_W K_{P1} T_W^2 T_{CO} / K_{P2} \\ b_2 = -0.5(K_W K_{P1} K_{I1} B_P - K_W^2 K_{P1} K_{I1}) T_W^2 \\ \quad - K_W K_{P1} T_{CO} / K_{P2} \\ \quad - 0.5(K_W K_{P1} K_{I1} B_P - K_W^2 K_{P1} K_{I1}) T_W^2 \\ \quad + 0.5K_W^2 K_{P1} K_{I1}^2 B_P T_{CO} T_W / K_{P2} \\ \quad - 1.5(K_W K_{P1} K_{I1} B_P - K_W^2 K_{P1} K_{I1}) T_W T_{CO} / K_{P2} \\ b_3 = (K_W K_{P1} K_{I1} B_P - K_W^2 K_{P1} K_{I1}) - 1.5K_W^2 K_{P1} K_{I1}^2 B_P T_W \\ \quad - K_W^2 K_{P1} K_{I1}^2 B_P T_{CO} / K_{P2} \end{cases}$$

According to the phase compensation method, the following equations should be satisfied.

$$\begin{cases} T_{GPSSD} = |G_{GPSS}G_{hm}| \cos(\phi + \gamma) = D_{GPSS} \\ T_{GPSSS} = |G_{GPSS}G_{hm}| \sin(\phi + \gamma) = 0 \end{cases} \tag{23}$$

It can be set that

$$\gamma = -\phi, \quad |G_{GPSS}| = \frac{D_{GPSS}}{|G_{hm}|}. \tag{24}$$

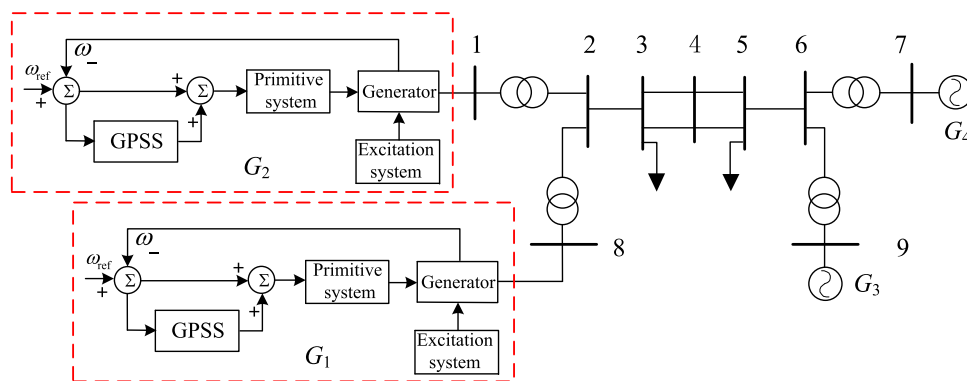
According to Eq. (15), the transfer function of GPSS can be written as

$$G_{GPSS}(s) = K_{GPSS1} \frac{1 + sT_2}{1 + sT_1} K_{GPSS2} \frac{1 + sT_4}{1 + sT_3} \tag{25}$$

where  $K_{GPSS} = K_{GPSS1} K_{GPSS2}$ . The GPSS parameters need to satisfy

$$\begin{cases} K_{GPSS1} \frac{1+j\omega_s T_2}{1+j\omega_s T_1} = |G_{GPSS}| \angle -\frac{\phi}{2} \\ K_{GPSS2} \frac{1+j\omega_s T_4}{1+j\omega_s T_3} = 1.0 \angle -\frac{\phi}{2} \end{cases} \tag{26}$$

Fig. 6 4-machine 2-area system



i.e.,

$$\begin{cases} K_{\text{GPSS}} = |G_{\text{GPSS}}| \frac{\sqrt{1+T_1^2} \sqrt{1+T_3^2}}{\sqrt{1+T_2^2} \sqrt{1+T_4^2}} \\ \arctan(\omega_S T_2) - \arctan(\omega_S T_1) = \arctan(\omega_S T_4) - \arctan(\omega_S T_3) = -\frac{\phi}{2} \end{cases} \quad (27)$$

which allows the GPSS to provide a positive damping torque. Since the connection between the governor system and the power grid is weak, the mechanical damping provided by the GPSS is not affected by the grid operating modes and conditions.

### 3.2.2 GPSS parameters tuning in multi-machine system

Due to the decoupled operation of the GPSS in the multi-machine system, the phase-compensation-based GPSS parameters tuning method in a single-machine system can be extended to the multi-machine system. The specific steps are as follows:

1. Based on the linearized state-space model of the multi-machine system in Eq. (8), together with Eqs. (9)–(11), the oscillation frequency  $\omega_S$  in ULFO mode and the damping ratio  $\zeta_S$  can be calculated;
2. With the given oscillation frequency  $\omega_S$ , the amplitude  $|G_{\text{hm}}|$  and phase angle  $\phi$  can be calculated from the system parameters and the oscillation frequency, according to Eqs. (21) and (22);
3. GPSS needs to provide a positive damping torque. According to the phase compensation principle, the GPSS design should satisfy Eq. (19), and parameter tuning should satisfy Eq. (24);
4. Given the desired damping torque coefficient  $D_{\text{GPSS}}$  from GPSS, which satisfies  $D_{\text{GPSS}} > |\zeta_S|$ , the transfer function of GPSS is rewritten as Eq. (25). At the same time, the time constants are set to  $T_1 = T_3$  and  $T_2 = T_4$ ;
5. According to Eq. (27), all the GPSS parameters can be calculated.

## 4 Analysis and examples

### 4.1 ULFO characteristics

According to the actual operating parameters of the 4-machine 2-area system, and based on the linearized state-space equation, the characteristic analysis method is used to study the ULFO problem.

#### 4.1.1 Verification of the linearized state-space model

The structure and steady-state data of the 4-machine 2-area system in Fig. 6 are derived from Ref. [11]. In the system,  $G_1$  and  $G_2$  are the hydropower units with GPSS,  $G_3$  and  $G_4$  are steam turbine units. GM\GM+, GA, and TW models are adopted for the hydropower governor control systems, while GS and TB models are used for the steam turbine governor control systems. The MG, FG, and constant power load models are adopted for the third-order generator, first-order excitation system, and the load, respectively. The dynamic parameter values for the MG models and the governor control system models of the four generators are shown in Table 1.

The PSD-BPA software is used to simulate the 4-machine 2-area system. The simulation time is set to 100 s. At  $t = 10$  s, a 3-phase short-circuit fault, which lasts for 0.1 s, occurs between lines 4 and 5. The simulations obtain the oscillations of the angular speed deviation of the generator before and after GPSS participation in Fig. 7.

In Fig. 7, the ULFO occurs in 10 s, and the 4 oscillation curves of the angular speed deviations are in phase completely. Prony is used to analyze the curves in Fig. 7. At the same time, based on the linearized state-space model of the multi-machine system, the oscillation frequency and damping ratio of the ULFO mode in the 4-machine 2-area system are calculated. The results are compared in Table 2. The consistent results endorse the linearized state-space model of the multi-machine system as an effective tool to analyze the oscillation characteristics of ULFO.

**Table 1** Model parameters

Parameter	Value	Parameter	Value
$M/s (G_1, G_2)$	6.5	$K_{GPSS} (G_2)$	0.0166
$M/s (G_3, G_4)$	6.175	$T_1 (G_2)$	0.40
$K_W (G_1, G_2)$	1.2	$T_2 (G_2)$	8.80
$K_{P1} (G_1, G_2)$	5.5	$T_3 (G_2)$	0.40
$K_{I1} (G_1, G_2)$	0.3	$T_4 (G_2)$	8.80
$T_{CO/s} (G_1, G_2)$	15.0	$R (G_3, G_4)$	0.05
$T_W/s (G_1)$	1.0	$T_C (G_3, G_4)$	0.5
$T_W/s (G_2)$	2.0	$F_{HP} (G_3, G_4)$	0.3
$K_{GPSS} (G_1)$	0.0434	$F_{IP} (G_3, G_4)$	0.7
$T_1 (G_1)$	0.50	$T_{CH} (G_3)$	0.3
$T_2 (G_1)$	5.82	$T_{CH} (G_4)$	0.4
$T_3 (G_1)$	0.50	$T_{RH} (G_3)$	8.0
$T_4 (G_1)$	5.82	$T_{RH} (G_4)$	5.0

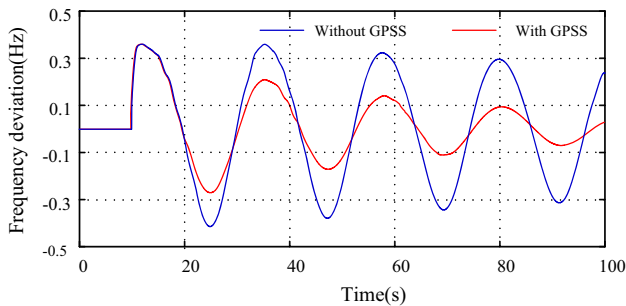


**Fig. 7** Oscillation of angular speed deviation in the 4-machine 2-area system

**Table 2** Identification results of Prony analysis and calculation results of the state-space model

Category	With or without GPSS	Frequency (Hz)	Damping ratio (%)
Prony analysis	Without GPSS	0.046	1.3
	With GPSS	0.046	6.8
State-space model	Without GPSS	0.046	0.7
	With GPSS	0.046	7.2

**4.1.2 Analysis of the mechanical damping torque coefficient**

Based on Eqs. (4) and (6), the phase–frequency curves of the hydropower and steam turbine governor control systems of the 4-machine 2-area system can be obtained (Fig. 8). The phase angle variations of  $-\Delta P_{hm}$  and  $-\Delta P_{sm}$  concerning  $\Delta\omega$  are presented, respectively.

From the phase–frequency curves shown in Fig. 8, when the oscillation frequency is 0.01–0.1 Hz (corresponding

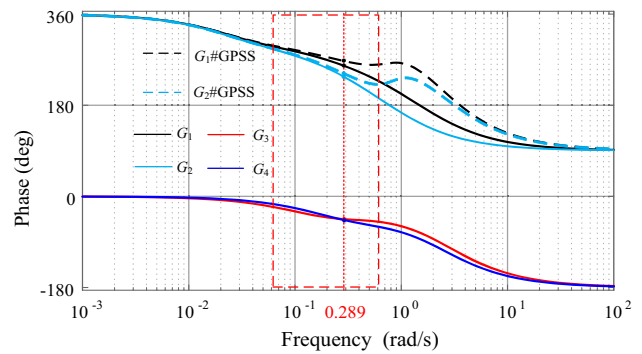


**Fig. 8** Phase–frequency curves of governor control system

**Table 3** Mechanical damping torque coefficients of  $G_1$ – $G_4$

Generator	Mechanical damping torque	Generator	Mechanical damping torque
GPSS ( $G_1$ )	– 0.623	GPSS ( $G_2$ )	– 1.35
GPSS ( $G_1$ )	– 0.139	GPSS ( $G_3$ )	6.732
GPSS ( $G_2$ )	– 1.787	GPSS ( $G_4$ )	8.364

angular frequency 0.0628–0.628 rad/s), the governor control systems of hydropower units  $G_1$  and  $G_2$  have larger phase lags than those of steam turbine units  $G_3$  and  $G_4$ . Without GPSS for  $G_1$  and  $G_2$ , the ULFO mode has  $\lambda_{1,2} = -0.002 \pm j0.286$ , the oscillation frequency is 0.046 Hz, and the phase lags of  $-\Delta P_{hm}$  in  $G_1$  and  $G_2$  and  $-\Delta P_{sm}$  in  $G_3$  and  $G_4$  concerning  $\Delta\omega$  are  $102^\circ$ ,  $124^\circ$ ,  $45^\circ$ , and  $46.7^\circ$ , respectively. Therefore, when ULFO occurs,  $\Delta\omega$  falls in the first quadrant, and the steam turbine governor control systems provide positive damping; but  $-\Delta P_{hm}$  falls in the 4th quadrant, and the hydropower governor control systems provide negative damping. With GPSS added to  $G_1$  and  $G_2$ , the ULFO mode has  $\lambda_{1,2} = -0.021 \pm j0.297$ , the oscillation frequency is still 0.046 Hz, and the phase lags of  $-\Delta P_{hm}$  in  $G_1$  and  $G_2$  concerning  $\Delta\omega$  are, respectively,  $93^\circ$  and  $118^\circ$ , which are lower than those without GPSS. Before and after the GPSS, the values of the mechanical damping torque coefficients of  $G_1$ – $G_4$  are shown in Table 3, which shows an increase in the mechanical damping torque coefficients after the GPSS involvement.

Equation (14) shows that the damping ratio  $\zeta_S$  of ULFO increases with the increase of the mechanical damping torque coefficient. Therefore, ULFO is mainly due to the negative mechanical damping torque coefficient of the hydropower governor control system in ultra-low-frequency range, which reduces  $\zeta_S$  to impair the system damping. The addition of GPSS in the hydropower governor control system can generate a leading phase to reduce the phase lag of  $-\Delta P_{hm}$  with respect to  $\Delta\omega$ , so that the increased mechanical damping torque coefficient of the governor control system as well as the system damping ratio could be helpful to suppress ULFO.



**Table 4** Participation factors of system models

Model	Participation factor	Model	Participation factor
MG ( $G_1$ )	1.5640	FG ( $G_2$ )	0.0021
GM ( $G_1$ )	0.0995	MG ( $G_3$ )	0.8100
GA ( $G_1$ )	0.6791	GS ( $G_3$ )	0.0653
TW ( $G_1$ )	0.3034	TB ( $G_3$ )	0.2854
FG ( $G_1$ )	0.0014	FG ( $G_3$ )	0.0004
MG ( $G_2$ )	1.8299	MG ( $G_4$ )	1.0919
GM ( $G_2$ )	0.1071	GS ( $G_4$ )	0.0790
GA ( $G_2$ )	0.7310	TB ( $G_4$ )	0.3619
TW ( $G_2$ )	0.5703	FG ( $G_4$ )	0.0005

**Table 5** Some parameters and its value ranges

Parameter	Value range	Parameter	Value range
$K_{P1}$	4.0–9.0	$K_{I1}$	0–1.0

**4.1.3 Sensitivity analysis of ULFO mode**

The participation factor reflects each state variable’s relative degree of involvement in the oscillation mode. A pair of conjugate eigenvalues of the ULFO mode is calculated with the linearized state-space model of the multi-machine system:  $\lambda_{1,2} = -0.010 \pm j0.290$ . Based on the left and right eigenvectors, the participation factors of the system model in ULFO are calculated (Table 4).

In Table 4, the MG, GM, GA, and TW models of hydropower units  $G_1$  and  $G_2$ , and the MG, GS, and TB models of steam turbine units  $G_3$  and  $G_4$  all take part in ULFO, while the FG models of the 4 generators hardly participate. For a constant power load, the state variable of the excitation system is completely decoupled from ULFO. The excitation system has a participation factor of 0 and does not participate in ULFO.

**4.1.4 Influence of governor system model parameters on eigenvalues**

Now, turn to the proportional gain ( $K_{P1}$ ) and integral gain ( $K_{I1}$ ) of the hydropower governor system model, for which reasonable value ranges are set, as shown in Table 5.

One of the parameters is made to increase monotonically within the range in Table 5, while other parameters and the operating mode are kept unchanged. The corresponding eigenvalues calculated by the linearized state-space model of the multi-machine system are plotted in Fig. 9.

From Fig. 9 and Eq. (11), the change of the damping ratio in response to an increase in a certain parameter is calculated and shown in Table 6. The PID parameters could be tuned

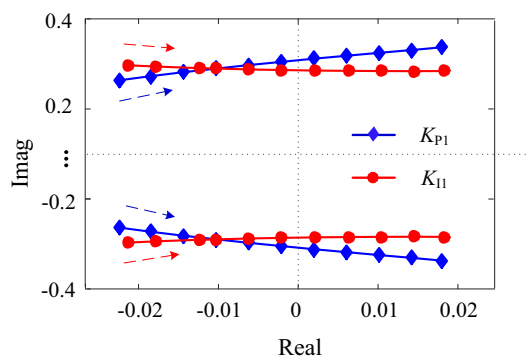


**Fig. 9** Root locus curves with different parameters

**Table 6** Change of damping ratio

Parameter	Damping ratio	Parameter	Damping ratio
$K_{P1}$	Decrease	$K_{I1}$	Decrease

within a reasonable range to raise the system damping ratio for ULFO suppression.

**4.2 Simulation verification of ULFO suppression by GPSS**

**4.2.1 Single-machine single-load system**

In the single-machine single-load system, the system parameters are set as  $M = 10.0$  s,  $K_W = 1.5$ ,  $K_{P1} = 3.8$ ,  $K_{I1} = 0.53$ ,  $B_P = 0.05$ ,  $K_{P2} = 3$ ,  $T_{CO} = 20$  s,  $T_2 = 0$  s, and  $T_W = 1.0$  s. The simulation time is set to 100 s. At  $t = 2$  s, the system has a 3-phase short-circuit fault, which lasts for 0.2 s. The simulation obtains the oscillations of angular speed deviation and mechanical power deviation, shown in Fig. 10. The calculated eigenvalues of the system are  $0.0000 \pm j0.3082$ . A ULFO with an angular speed oscillation period of 20.384 s and oscillation amplitude 0.1 Hz is generated in the system.

From Eqs. (21) and (22),  $|G_m| = 1.004$  and  $\phi = 109.6^\circ$ , that is,  $\Delta P_m$  lags  $-\Delta\omega$  by  $109.6^\circ$ . If the GPSS is added to the governor control system to increase the system mechanical power damping by 0.142, one should set  $D_{GPSS} = -0.142$ . The calculated parameters of the designed GPSS are  $K_{GPSS} = 0.7766$ ,  $T_1 = T_3 = 0.592$  s, and  $T_2 = T_4 = 7.0$  s. Using these parameter values, the oscillation curves of the angular speed deviation with and without the GPSS are obtained, as shown in Fig. 11.

After calculation, the eigenvalues of the system with GPSS are  $\lambda_{1,2} = -0.0442 \pm j0.3082$ . From Fig. 11, without GPSS, the system is zero-damping with a ULFO of constant amplitude, as the negative damping provided by the governor control system and the positive damping in the system cancel out each other. With GPSS added, GPSS reduces the negative damping by the governor control system to pull the system

**Fig. 10** Oscillations of angular speed deviation and mechanical power deviation

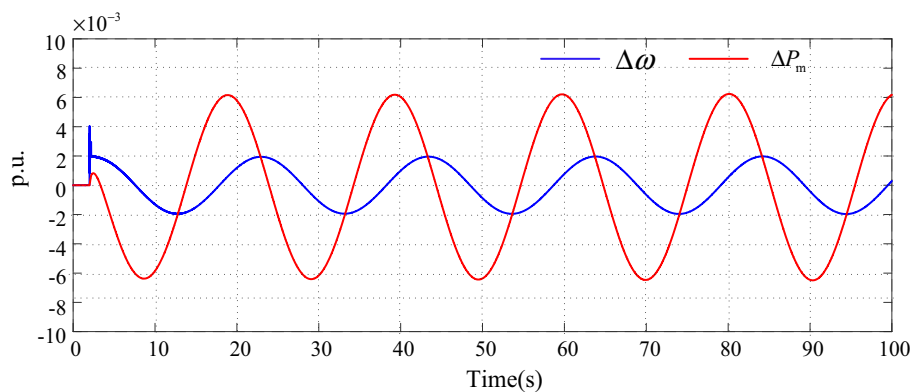
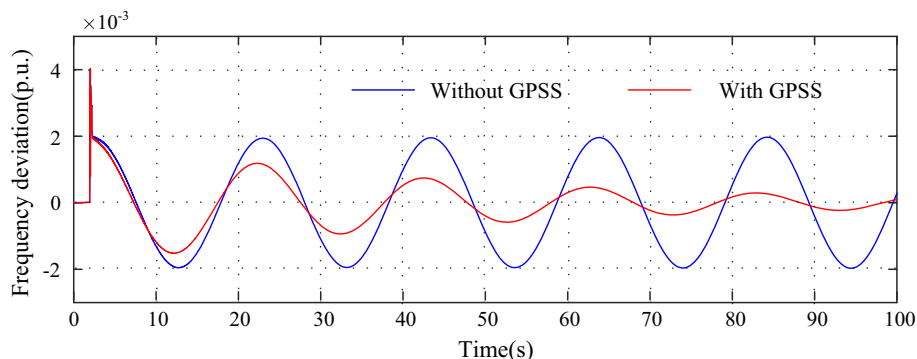


**Fig. 11** Oscillations of angular speed deviation in the single-machine single-load system



into a positive damping state, so that the ULFO gradually dies out.

### 4.2.2 Actual power grid

When ULFO occurs in a system, all the generator units oscillate synchronously. To study the close relationship between the hydropower units and ULFO in the Yunnan power grid, the frequency regulation effect of the thermal power units and the minor hydropower plants is neglected. Based on the offline simulation result of Yunnan power grid in 2017, 13 large capacity hydropower plants are selected as concerned objects: Xiaowan (XW), Jinanqiao (JAQ), Xiluodu (XLD), Zhazadu (NZD), Manwan (MW), Dachaoshan (DCS), Gongguoqiao (GGQ), Jinghong (JH), Longkou (LKK), Ahhai (AH), Ludila (LDL), Liyuan (LY), and Guanyinyan (GY). The simulation is to verify the effectiveness of GPSS for ULFO suppression. When a constant amplitude ULFO occurs, the main parameters of the governor systems of 13 main hydropower plants are shown in Table 7, in which  $K_i$  is the ratio of the rated capacity of the  $i$ th hydropower plant over the total capacity of the 13 main hydropower plants.

During the GPSS parameter setup for the Yunnan power grid simulation system, each of the 13 main hydropower plants is equipped with a GPSS that is supposedly providing the same damping torque coefficient. The GPSS parameters are designed with the phase compensation method. The sim-

**Table 7** Main parameters of the governor systems of 13 main hydropower plants

Hydropower plant	$S$	$K_P$	$K_I$	$K_D$	$B_P$	$T_W$ (s)	$K_i$
XW	$6 \times 778$	5.0	3.00	1.0	0.04	3.0	0.11
JAQ	$4 \times 667$	5.0	3.00	1.0	0.04	3.0	0.06
XLD	$9 \times 856$	5.0	3.00	1.0	0.04	3.0	0.19
NZD	$9 \times 722$	5.0	3.00	1.0	0.04	3.0	0.16
MW	2801	2.0	0.63	1.0	0.04	3.0	0.07
DCS	$6 \times 250$	4.0	0.05	0.0	0.04	3.0	0.04
GGQ	$4 \times 250$	3.0	1.00	0.0	0.04	2.3	0.02
JH	$5 \times 389$	1.5	0.25	0.0	0.04	3.0	0.05
LKK	$5 \times 400$	2.5	0.50	3.0	0.04	3.6	0.05
AH	$5 \times 444$	5.0	3.00	1.0	0.04	4.0	0.05
LDL	$6 \times 400$	2.5	0.50	1.0	0.04	3.0	0.06
LY	$4 \times 667$	2.0	0.38	1.0	0.04	2.8	0.06
GY	$5 \times 667$	2.5	0.50	1.0	0.04	3.0	0.08

ulation time is set to 100 s. At 1 s, there is a three-phase short-circuit fault, which lasts for 0.2 s. The oscillation curves of the angular speed deviation with and without the GPSS are obtained by the simulation (Fig. 12). Prony analysis is performed on these curves, and a comparison is given in Table 8.

It can be seen from Fig. 12 and Table 8 that after GPSS is added, the oscillation amplitude of the angular speed deviation is gradually attenuated, and the damping ratio is raised

**Fig. 12** Oscillations of angular speed deviation in the actual power grid

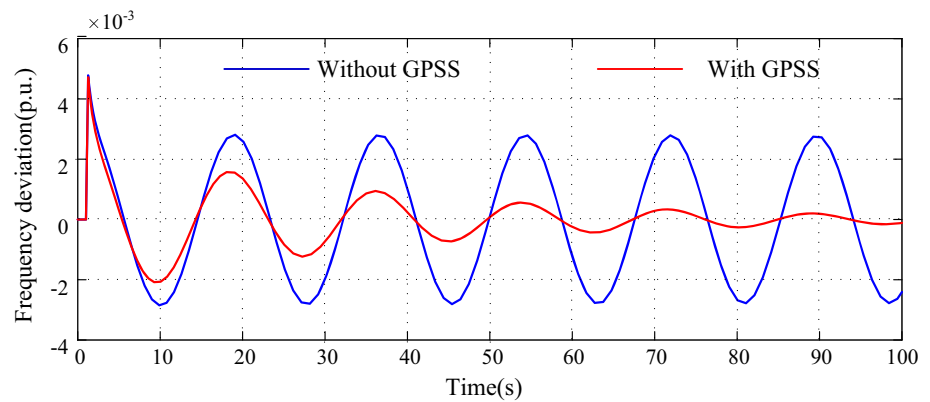


**Table 8** Comparison of oscillation modes

Without GPSS		With GPSS		Damping ratio increment %
Frequency (Hz)	Damping ratio (%)	Frequency (Hz)	Damping ratio (%)	
0.056	0.2	0.056	10.7	10.5

by 0.105. Therefore, adding GPSS to a multi-machine system can effectively suppress ULFO in the system.

## 5 Conclusions

In this paper, by establishing the linearized state-space model of a multi-machine system with PID-type governors, the characteristic analysis method is used to study characteristics and suppression measures of hydropower-unit-induced ULFO with the participation factors and root locus. The conclusions are as follows:

1. The governor control system model places a part in ULFO, while the excitation system model does not. In Table 4, the MG, GM, GA, and TW models of hydropower units  $G_1$  and  $G_2$ , as well as the MG, GS, and TB models of steam turbine units  $G_3$  and  $G_4$  in the 4-machine 2-area system all have large participation factors, while the participation factor of the excitation system is 0.
2. With the increase in proportional gain  $K_{P1}$  and integral gain  $K_{I1}$  of the PID-type governor system, the system damping ratio is gradually reduced. In Fig. 4 with the increase of  $K_{P1}$  and  $K_{I1}$  in the 4-machine 2-area system, the real part of the eigenvalues of the ULFO mode gradually increases, and the system damping ratio gradually deteriorates.
3. The GPSS with leading phase element is added on the governor side, and the GPSS transfer function is divided into leading and lag elements—both with gains. By properly setting the parameters in each part, the phase lag generated by the complicated hydropower governor

system can be compensated, and the desired positive damping torque achieved, to suppress ULFO in the system.

**Acknowledgements** This work is supported by the China Southern Grid Project (No. K-YNKJXM-20160159) and the National Natural Science Funds of China (No. 51477143).

## Compliance with ethical standards

**Conflict of interest** The authors have declared that they have no conflict of interest.

## References

1. Liu Z, Yao W, Wen J (2017) Enhancement of power system stability using a novel power system stabilizer with large critical gain. *Energies* 10:449
2. Shim K-S, Ahn S-J, Choi J-H (2017) Synchronization of low-frequency oscillation in power systems. *Energies* 10:558
3. Shim K-S, Ahn S-J, Yun S-Y, Choi J-H (2017) Analysis of low-frequency oscillation using the multi-interval parameter estimation method on a rolling blackout in the KEPCO system. *Energies* 10:484
4. Yang W, Yang J, Guo W, Zeng W, Wang C, Saarinen L, Norlund P (2015) A mathematical model and its application for hydro power units under different operating conditions. *Energies* 8:10260–10275
5. Cebeci ME, Karaağaç U, Tör OB et al (2007) The effects of hydropower plants' governor settings on the stability of Turkish power system frequency. In: 5th International conference on electrical and electronics engineering, Bursa, Turkey
6. Villegas HN (2011) Electromechanical oscillations in hydro-dominant power systems: an application to the Colombian power system. Graduate Theses and Dissertations. Iowa State University, Ames, Iowa

7. Dandeno Kundu PP, Bayne J (1978) Hydraulic unit dynamic performance under normal and islanding conditions—analysis and validation. *IEEE Trans Power Appar Syst PAS* 97(6):2134–2143
8. Pico HV, McCalley JD, Angel A et al (2012) Analysis of very low-frequency oscillations in hydro-dominant power systems using multi-unit modeling. *IEEE Trans Power Syst* 27(4):1906–1915
9. Gong TR, Wang GH, Li T et al (2014) Analysis and control on ultra-low frequency oscillation at seeding end of UHVDC power system. In: *Proceedings of international conference of IEEE power system technology*, pp 832–837
10. Mo WK, Chen YP, Chen HY et al (2017) Analysis and measures of ultra-low-frequency oscillations in a large-scale hydropower transmission system. *IEEE J Emerg Sel Top Power Electron* 6:1077–1085
11. Kundur P (1994) *Power system stability, and control*. McGraw-Hill, New York
12. Teng YF, Zhang P, Han Y et al (2018) Mechanism and characteristics analysis of ultra-low frequency oscillation phenomenon in a power grid with a high proportion of hydropower. In: *International conference on power system technology*, pp 1–6
13. Zheng C, Ding GQ, Liu BS et al (2018) Analysis and control to the ultra-low frequency oscillation in southwest power grid of China: a case study. In: *Chinese control and decision conference, Shenyang, China*
14. Hu W, Liang J, Jin Y, Wu F, Wang X, Chen E (2018) Online evaluation method for low-frequency oscillation stability in a power system based on improved XGboost. *Energies* 11:3238
15. Wang GT, Xu Z, Guo XY et al (2018) Mechanism analysis and suppression method of ultra-low-frequency oscillations caused by hydropower units. *Int J Elect Power Energy Syst* 103:102–114
16. Jiang CX, Zhou JH, Shi P et al (2019) Ultra-low frequency oscillation analysis and robust fixed order control design. *Int J Elect Power Energy Syst* 104:269–278
17. Zeng D, Zheng Y, Luo W, Hu Y, Cui Q, Li Q, Peng C (2019) Research on improved auto-tuning of a PID controller based on phase angle margin. *Energies* 12:1704
18. Özdemir MT, Öztürk D (2017) Comparative performance analysis of optimal PID parameters tuning based on the optics inspired optimization methods for automatic generation control. *Energies* 10:2134
19. Ding T, Chang L, Li C, Feng C, Zhang N (2018) A mixed-strategy-based whale optimization algorithm for parameter identification of hydraulic turbine governing systems with a delayed water hammer effect. *Energies* 11:2367
20. Demello FP, Koessler RJ, Agee J, Anderson PM, Doudna JH, Fish JH, Hamm PA, Kundur P, Lee DC, Rogers GJ, Taylor C (1992) Hydraulic turbine and turbine control models for system dynamic studies. *IEEE Trans Power Syst* 7(1):167–179. <https://doi.org/10.1109/59.141700>
21. Yu X, Zhang J, Fan C, Chen S (2016) Stability analysis of governor turbine-hydraulic system by state space method and graph theory. *Energy* 114:613–622
22. Liu Z, Yao W, Wen J, Cheng S (2018) Effect analysis of generator governor system and its frequency mode on inter-area oscillations in power systems. *Int J Elect Power Energy Syst* 96:1–10
23. Chen G, Tang F, Shi HB et al (2017) Optimization strategy of hydro-governors for eliminating ultra-low frequency oscillations in hydro-dominant power systems. *IEEE J Emerg Sel Top Power Electron* 6(3):1086–1094
24. Chen L, Lu XM, Min Y et al (2018) Optimization of governor parameters to prevent frequency oscillations in power systems. *IEEE Trans Power Syst* 33(4):4466–4474
25. Ju X, Zhao P, Sun H, Yao W, Wen J (2017) Nonlinear synergetic governor controllers for steam turbine generators to enhance power system stability. *Energies* 10:1092
26. Schleif FR, Martin GE, Angell RR et al (1967) Damping of system oscillations with hydro generator unit. *IEEE Trans Power Appar Syst* 86(4):438–442
27. Gao B, Xia C, Chen N, Cheema KM, Yang L, Li C (2017) Virtual synchronous generator based auxiliary damping control design for the power system with renewable generation. *Energies* 10:1146
28. Zhou T, Chen Z, Bu S, Tang H, Liu Y (2018) Eigen-analysis considering time-delay and data-loss of WAMS and ITS application to WADC design based on damping torque analysis. *Energies* 11:3186
29. Mayouf F, Djahli F, Mayouf A et al (2013) Study of excitation and governor power system stabilizers effect on the stability enhancement of a single machine infinite bus power system. In: *IEEE international conference on environment and electrical engineering, Wroclaw, Poland*
30. Zhang WL, Xu F, Hu W et al (2012) Research of coordination control system between nonlinear robust excitation control and governor power system stabilizer in multi-machine power system. In: *IEEE international conference on power system technology (POWERCON), Auckland*
31. Paul DFV, Malik OP et al (2014) Adaptive damping controller for a superconducting generator. In: *IEEE power India international conference, Delhi, India*

**Publisher's Note** Springer Nature remains neutral with regard to jurisdictional claims in published maps and institutional affiliations.